Fish and Shellfish Immunology 95 (2019) 481–490

Contents lists available at ScienceDirect

Fish and Shellfish Immunology

journal homepage: www.elsevier.com/locate/fsi

Full length article

Integrated dual RNA-seq and dual iTRAQ of infected tissue reveals the functions of a diguanylate cyclase gene of *Pseudomonas plecoglossicida* in host-pathogen interactions with *Epinephelus coioides*

Gang Luo[a,c], Lingmin Zhao[a], Xiaojin Xu[a], Yingxue Qin[a], Lixing Huang[a], Yongquan Su[b], Weiqiang Zheng[b], Qingpi Yan[a,b,*]

[a] Fisheries College, Jimei University, Xiamen, Fujian, 361021, PR China
[b] State Key Laboratory of Large Yellow Croaker Breeding, Ningde, Fujian, 352000, PR China
[c] Hubei Key Laboratory of Cell Homeostasis, College of Life Sciences, Wuhan University, Wuhan, Hubei, 430072, PR China

ARTICLE INFO

Keywords:
Host-pathogen interactions
Epinephelus coioides
Pseudomonas plecoglossicida
Dual RNA-Seq
Dual iTRAQ
Diguanylate cyclase gene

ABSTRACT

The interactions between host and pathogen is exceedingly complex, which involves alterations at multiple molecular layers. However, research to simultaneously monitor the alterations of transcriptome and proteome between a bacterial pathogen and aquatic animal host through integrated dual RNA-seq and dual iTRAQ of tissue during infection is currently lacking. The important role of a diguanylate cyclase gene (*L321_RS15240*) in pathogenicity of *Pseudomonas plecoglossicida* against *Epinephelus coioides* was suggested by previous dual RNA-seq of our lab. Then *L321_RS15240*-RNAi strains of *P. plecoglossicida* were constructed with pCM130/tac, and the mutant with the best silencing effect was selected for follow-up study. The RNAi of *L321_RS15240* resulted in a significant decrease in bacterial virulence of *P. plecoglossicida*. The *E. coioides* spleens infected by wild type strain or *L321_RS15240*-RNAi strain of *P. plecoglossicida* were subjected to dual RNA-seq and dual iTRAQ, respectively. The results showed that: RNAi of *L321_RS15240* led to 1)alterations of host transcriptome associated with complement and coagulation cascades, ribosome, arginine and proline metabolism, and oxidative phosphorylation; 2)high expression of host proteins which related to phagosome and metabolism responses (metabolism of glutathione, amino sugar and nucleotide sugar); 3)the highly differentially expression of host lncRNAs and miRNAs. The differentially expressed proteins and mRNAs of pathogen were different after infection, but the functions of these proteins and mRNAs were mainly related to metabolism and virulence. This study provides a new insight to comprehensively understand the gene functions of pathogens and hosts at multiple molecular layers during *in vivo* infection.

1. Introduction

Once infection occurs, both the pathogen and the host should try to attack each other and protect themselves [1]. Pathogen-host interactions determine the course and final result of the disease [2]. Understanding the mechanism of pathogen-host interaction is especially important for revealing pathogenesis as well as prevention and treatment of disease [3]. Over the past decade, omic approaches have emerged as powerful tools for understanding pathogenesis at the molecular level [4].

For bacterial pathogen interactions with eukaryotic host, transcriptomic studies were long technically limited to analyzing gene expression in either bacteria or infected host [5,6]. To gain a deeper understanding of the underlying pathogenic mechanisms, a thought experiment in 2012 proposed that it's possible to simultaneously monitor pathogen and host transcriptomes by using dual RNA-seq in bacterial infection biology [5]. Recently, dual RNA-seq analyses for pathogen-host interactions were used successfully in lung epithelial cells infected with *Streptococcus pneumoniae* [7], tissue infected samples [8], and the roles of a single virulence gene in host-pathogen interactions [9,10].

Proteomic approaches are also introduced to the understanding of host-pathogen interactions [4]. When studying the bacterial pathogen-host interactions, because of overall much lower levels of bacterial proteins in host, simultaneous analysis of both bacterial and host proteomes is highly challenging during infection, especially *in vivo* models

* Corresponding author. Fisheries College, Jimei University, Xiamen, Fujian, 361021, PR China.
E-mail address: yanqp@jmu.edu.cn (Q. Yan).

https://doi.org/10.1016/j.fsi.2019.11.008
Received 5 October 2019; Received in revised form 30 October 2019; Accepted 2 November 2019
Available online 04 November 2019
1050-4648/

[11]. Recently, label-free quantitative MS were used successfully for simultaneous characterization of the bacterial and host proteomes in a small tissue [12]. The current technological advances make isobaric tags for relative and absolute quantitation (iTRAQ)-based proteomic analysis more accurate and sensitivity than label-free quantitative MS [13]. The advantages of iTRAQ technique provide a potential platform for dual characterization of the bacterial and host proteomes of *in vivo*. Thus, it is possible for us to simultaneous analysis of transcript and protein profiles of bacteria and host by using integrated dual RNA-seq and iTRAQ of tissue.

Both the tissue dual RNA-seq and dual proteomic provide specific insights for reflecting the complexities of the *in vivo* infection. While all previous studies have their limitations. The interactive relationship between a pathogen and its host is exceedingly complex, which involves alterations at multiple molecular layers (e.g., RNA transcripts, proteins, and metabolites) [2,9]. Furthermore, these layers are interconnected and complementing each other [9]. However, all these previous studies discussed pathogen-host interactions at a single molecular layer. The mRNAs and proteins levels are not always in consistent, whereas proteins are the direct performers of body functions and provide more direct evidence [14,15]. Therefore, an overall association analysis of transcriptome and proteome will deepen the understanding of pathogen-host interaction. However, related research has not been reported at present.

Pseudomonas plecoglossicida, a Gram-negative bacterium, has been frequently associated with some animals of economic importance and leads to high mortality [16–18]. Diguanylate cyclases (DGCs) containing the GGDEF domain can catalyze synthesis of cyclic di-GMP (c-di-GMP) [19]. C-di-GMP is one of the most common and important bacterial second-messenger molecules, which has been shown to regulate the cell cycle, biofilm formation, motility, virulence, differentiation, and other cellular functions [20]. In our previous study, artificial infection of the *P. plecoglossicida* in *Epinephelus coioides* results in numerous white nodules in spleen and causes high mortality about at 18 °C but not 28 °C (normal growth temperature of *P. plecoglossicida*). Futher RNA-seq for the wild *P. plecoglossicida* cultured at the two temperatures showed that *L321_RS15240* (a diguanylate cyclase gene) was one of the highest expression levels of all genes to strain cultured at 18 °C than 28 °C. Therefore, *L321_RS15240* was hypothesized to play an important role in the pathogenicity of *P. plecoglossicida.* But, there is no report on the function of diguanylate cyclase gene in host pathogen interaction.

This study, to the best of our knowledge, for the first time to study the pathogen-host interaction at dual molecular layers by integrated dual RNA-Seq and dual proteomic of tissue, and the first time introducing iTRAQ to tissue dual proteomic study. The goal of this work is to provide a novel insight truly reflecting of the complexity of host-pathogen interaction *in vivo*, and elucidate the function of a diguanylate cyclase in *P. plecoglossicida*.

2. Materials and methods

2.1. Bacterial strains and culture conditions

The pathogenic *P. plecoglossicida* (NZBD9) was isolated from the spleen of naturally infected large yellow croaker (*Pseudosciaena crocea*) [21]. The *P. plecoglossicida* strain was routinely grown in LB (Luria Bertani) broth at 18 or 28 °C with shaking at 220 rpm. *Escherichia coli* DH5α was obtained from TransGen Biotech (Beijing, China), which was grown in LB broth (37 °C, 220 rpm).

2.2. Construction of P. plecoglossicida RNAi strain

RNAi strain was constructed according to methods described by Zhang et al. [22]. Five short hairpin RNA sequences targeting the *L321_RS15240* gene were designed and synthetized (Supplementary Table 1). After linearizing pCM130/tac vectors with the restriction enzymes *Nsi*I and *Bsr*GI (New England Biolabs), the oligonucleotides were annealed and ligated to the linearized pCM130/tac vectors using T4 DNA ligase (New England Biolabs) following the manufacturer's recommendations. The recombinant pCM130/tac vectors were transformed into the competent *E. coli* DH5a cells by heat shock and then were electroporated into *P. plecoglossicida* as described previously [23]. *P. plecoglossicida* with empty plasmid pCM130/tac was constructed as the control strain. Finally, the expression level of *L321_RS15240* of each RNAi strain was detected by qRT-PCR.

2.3. Artificial infection and sampling

All animal experiments were follow the 'Guide for the Care and Use of Laboratory Animals' set by the National Institutes of Health. The animal protocols were approved by the Animal Ethics Committee of Jimei University (Acceptance NO JMULAC201159).

Healthy *E. coioides* were obtained from Zhangzhou (Fujian, China) and were acclimatized at 18 °C for one week under specific pathogen-free laboratory conditions. For survival assays, 60 weight-matched *E. coioides* were intrapleurally injected with 10^3 *cfu/g* of *P. plecoglossicida* (wild-type strain with the empty plasmid or the RNAi strain). 60 individual of *E. coioides* that were intrapleurally injected with PBS were used as a negative control. The water temperature during infection was 18 °C. The daily mortality of infected *E. coioides* was recorded. For tissue dual RNA-seq and iTRAQ assays, the spleens of six weight-matched *E. coioides* infected with wild-type *P. plecoglossicida* with an empty plasmid or the RNAi strain were sampled at 24 h post infection (hpi). Every two spleens were mixed as one sample. For the tissue distribution assays, the spleens, livers, head kidneys, trunk kidneys and blood of three weight-matched *E. coioides* were sampled at 6 and 12 hpi, and at 1, 2, 3, 4 and 5 day post injection (dpi).

2.4. DNA isolation

DNA purification from spleens, livers, head kidneys and trunk kidneys was accomplished with an EasyPure Marine Animal Genomic DNA Kit (TransGen Biotech, Beijing, China) following the manufacturer's instructions. The EasyPure Blood Genomic DNA Kit (TransGen Biotech) was used for DNA isolation from blood samples.

2.5. Digital PCR

Digital PCR (dPCR) was performed using the QuantStudio™ 3D Digital PCR System (Life Technologies, Carlsbad, CA, USA). Reaction mixtures (14.5 μL/QuantStudio 3D Digital PCR 20 K Chip) were comprised of 7.25 μL Digital PCR Master Mix (Life Technologies), 900 nM of the forward primer, 900 nM of the reverse primer, 250 nM TaqMan MGB probe (Life Technologies), 3 μL diluted template DNA and 1.25 μL of nuclease-free water. The primers and the TaqMan MGB probe sequences were as previously described [24]. Loaded chips were put into a Proflex PCR System (Life Technologies) for amplification and were imaged by the QuantStudio™ 3D Instrument (Life Technologies). The analyses were carried out using the Quantstudio™ 3D AnalysisSuite software (Life Technologies). The copy number of the *gyrB* gene was used to estimate *P. plecoglossicida* abundance, which were calculated as: (Copies/μL × 14.5 μL × dilution times)/(3 μL × mg/μL).

2.6. RNA isolation

Total RNA was extracted using TRIzol reagent (Invitrogen, Carlsbad, CA, USA) according to the manufacturer's instructions, the mixed genomic DNA in total RNA was digested with the Turbo DNA-free DNase (Ambion, Austin, TX, USA). The RNA quality was assessed using an Agilent 2100 Bioanalyzer (Agilent Technologies, Santa Clara, CA, USA), while the rRNA in total RNA was removed using the Ribo-Zero

rRNA Removal Kit (Epicentre, Madison, WI, USA) according to the manufacturer's instructions.

2.7. qRT-PCR

qRT-PCR was carried out using a QuantStudio 6 Flex (Life Technologies). All primer sequences are provided in Supplementary Tables 2–5. The expression of bacterial genes was normalized using *gyrB*. In *E. coioides*, the expression of mRNA and lncRNA was normalized to *β-actin,* and the miRNA expression was normalized by using *5S rRNA* gene [25]. The $2^{-\Delta\Delta Ct}$ method was used to calculate the relative level of gene expression.

2.8. Transcriptomic analysis

2.8.1. Library preparation and sequencing

The RNA-seq libraries were prepared using protocols supplied with the TruSeq™ RNA sample preparation Kit (Illumina, San Diego, CA, USA). In brief, the rRNA-depleted RNA sample was fragmented in fragmentation buffer, and cDNA synthesis was conducted using a SuperScript double-stranded cDNA synthesis kit (Invitrogen, Carlsbad, CA, USA). After end reparation, phosphorylation and poly (A) addition, the cDNA library was amplified using Phusion DNA polymerase (NEB). Small RNA-seq libraries were built using a TruSeqTM Small RNA Sample Prep Kit (Illumina) according to the manufacturer's instructions. An Agilent 2100 Bioanalyzer (Agilent Technologies) was used to validate the library quality. Sequencing was performed on the Illumina HiSeq4000 sequencing platforms at Majorbio Biotech Co., Ltd. (Shanghai, China).

2.8.2. Processing and mapping of reads

The trimming and quality control of raw Illumina reads were performed using Sickle (https://github.com/najoshi/sickle) and SeqPrep (https://github.com/jstjohn/SeqPrep) with the default settings. For RNA-seq, clean data were mapped to the genome of *P. plecoglossicida* strain NB2011 (NCBI RefSeq accession numbers: NZ_ASJX00000000.1) using Bowtie2 [26]. Mapped reads were classified as reads of *P. plecoglossicida*, and leftover reads were used for de novo assembly to obtain the *E. coioides* unigenes.

2.8.3. De novo assembly, detection of lncRNAs and annotation of mRNAs in the host

All clean reads, which were not mapped to the *P. plecoglossicida* genome from the wild-type and RNAi strain infected spleens, were treated as a pool of reads. This pool of reads was assembled de novo into unigenes using Trinity [27]. To remove any possible prokaryote contamination, all unigenes were first aligned to the bacterial NCBI non-redundant (NR) protein database. Next, the detection of lncRNAs was performed as described earlier [28]. For annotation of mRNAs, the clean unigenes were compared against different databases, including NCBI NR protein, STRING, SWISS-PROT and KEGG (Kyoto Encyclopedia of Genes and Genomes) databases using BLASTX to identify the proteins that shared the greatest sequence similarity with the identified unigenes. Gene Ontology (GO) annotations were conducted using the Blast2GO software (http://www.blast2go.com/b2ghome) [29]. Finally, KEGG was used for metabolic pathway analysis (http://www.genome.jp/kegg/).

2.8.4. Identification of miRNAs

The raw reads were processed through quality control to obtain clean reads. The clean reads were then blasted against the Rfam database (http://Rfam.sanger.ac.uk/) to annotate the miscellaneous RNAs. After filtering rRNA, snoRNA, scRNA, tRNA, snRNA and other non-coding RNA, the remaining sRNAs were mapped to the zebrafish miRNA data of miRBase version 21.0 to detect the known and new miRNAs.

2.8.5. Analysis of differential gene expression and functional enrichment of gene

The measurement of differential gene expression was performed individually for libraries of *P. plecoglossicida* and *E. coioides*. Expression analyses of transcriptome data from *P. plecoglossicida* and *E. coioides* were performed on the basis of annotations from NCBI (NZ_ASJX00000000.1) and the reference transcriptome annotation described above (annotation for the host transcriptome), respectively. After obtaining uniquely mapped read counts, the package edgeR (targeting mRNAs of host-pathogen and lncRNAs of host) [30] and DESeq2 (targeting miRNAs of host) [31] were used to test for differentially expressed genes (DEGs), which were determined by the following thresholds: $|\log2^{\text{fold change}}| \geq 0.6$ and P-value < 0.05 (for mRNAs of pathogen and miRNAs of host) [32]; $|\log2^{\text{fold change}}| \geq 1$ and a false discovery rate (FDR) < 0.05 (for mRNAs and lncRNAs of host). All differentially expressed mRNAs *(DEMs) of host* were used to for GO and KEGG enrichment analysis.

2.9. Proteomic analysis

2.9.1. iTRAQ assays

iTRAQ assays were carried out mainly based on methods described by Ouyang et al. [33]. In brief, total protein was extracted from spleen tissues by using a urea lysis buffer (7 M urea, 2 M thiourea, and 1% SDS) with a protease inhibitor. Protein concentrations were detected with a BCA Protein Assay Kit (Pierce, Thermo, USA). Following reduction, cysteine alkylation, and digestion, samples were labeled with iTRAQ Reagents Multiplex Kits according to the manufacturer's instructions (AB Sciex Inc., CA, USA). After being desalted with a C18 solid-phase extraction, peptides were used for Nano Liquid Chromatography–Mass Spectrometry/Mass Spectrometry (LC-MS/MS) analysis.

2.9.2. iTRAQ data analysis

The MS/MS data were searched using the Proteome Discoverer software version 2.1 (Thermo Fisher Scientific, San Jose, CA, USA) against the Uniprot database (*P. plecoglossicida* NB2011),and the protein database which were translated from the transcriptome data of *E. coioides* in this study. False discovery rate (FDR) of peptide identification was set as FDR ≤ 0.01. A minimum of one unique peptide identification was used to support protein identification. Annotation of all identified proteins was performed using GO (http://www.blast2go.com/b2ghome) and KEGG pathway (http://www.genome.jp/kegg/).

The thresholds of fold change (> 1.2 or < 0.83) and P-value < 0.05 were used to identify differentially expressed proteins (DEPs) [34]. DEPs were further used to for GO and KEGG enrichment analysis. Protein-protein interaction analysis was performed using the String v10.0 [35]. DEPs were compared with the *DEMs to* identify proteins that were consistently expressed at the mRNA level.

2.10. Statistical analyses

All data are expressed as the means ± standard deviation (SD) from at least three sets of independent experiments. Data analysis was performed using the SPSS 17.0 software (Chicago, IL, USA), and one-way analysis of variance with Dunnett's test were used. P values < 0.05 were considered statistically significant.

2.11. Data access

The RNA sequencing reads data were submitted to NCBI database under the accession numbers PRJNA563518, PRJNA564900, SRP114910 and SRP115064.

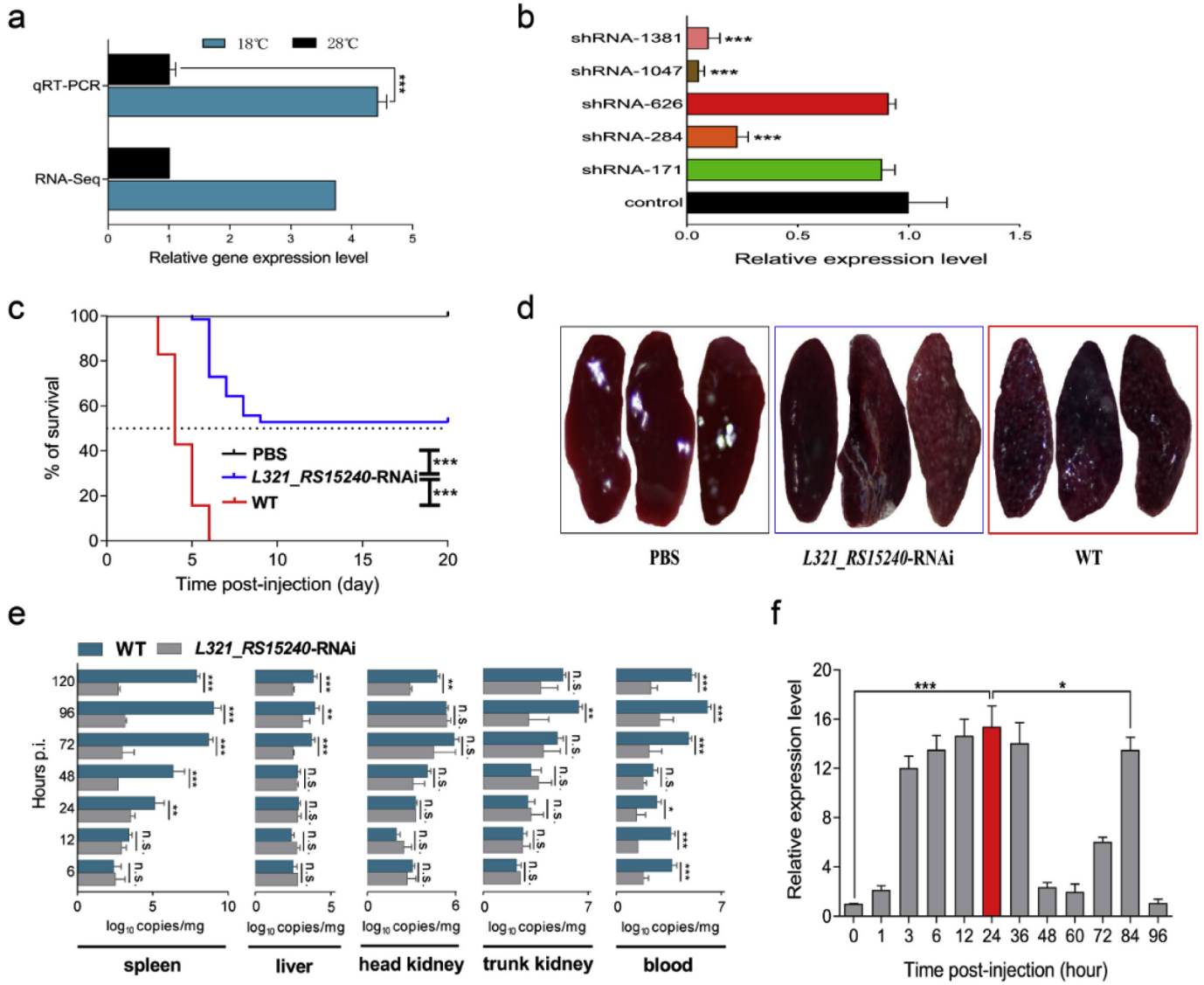

Fig. 1. The effects of the *L321_RS15240* gene on the pathogenicity of *P. plecoglossicida* in *E. coioides*. **a**, qRT-PCR validation of *L321_RS*15240 RNA-seq in *P. plecoglossicida* cultured at 18 °C and 28 °C. **b**, Screening of shRNAs targeting *L321_RS15240* transcript. **c**, *E. coioides* were intrapleurally injected with 10^3 cfu/g of *P. plecoglossicida* (WT strain containing empty plasmid, RNAi strain) or PBS. Survival of *E. coioides* was monitored for 20 d (n = 60 per group). (Mantel-Cox log-rank test). **d**, Representative photographs of spleens (4dpi) in *E. coioides* which were intrapleurally injected with 10^3 cfu/g of WT, RNAi strain and PBS. **e**, The dynamic distribution of RNAi strain in host. *E. coioides* were intrapleurally injected with 10^3 cfu/g of WT *P. plecoglossicida* strain containing empty plasmid, RNAi strain, respectively. The *E. coioides* were sacrificed 6 h, 12 h, 1d, 2d, 3d, 4d and 5d post-injection, and the numbers of bacteria in spleen, liver, head kidney, trunk kidney and blood was determined using dPCR. **f**, Detection of the *L321_RS15240* highest expression of WT *P. plecoglossicida* in infected spleens at 18 °C. Data are shown as means ± SD from three independent biological replicates. n.s., not significant; $*P < 0.05$, $**P < 0.01$, $***P < 0.001$.

3. Results

3.1. The effects of the L321_RS15240 gene on the pathogenicity of P. plecoglossicida to E. coioides

The results of qRT-PCR showed that *L321_RS15240* gene was significantly high expression at 18 °C than at 28 °C, which was consistent with the results of RNA-seq (Fig. 1a).

The stably silenced results showed that different shRNAs resulting in different knockdown efficiencies on *L321_RS15240* gene (Fig. 1b). The strain containing pCM130/tac-*L321_RS*15240-shRNA-1047 (named the *L321_RS15240*-RNAi strain) exhibited the best efficiency of gene silencing, and was chosen for further studies.

Compared with the counterparts injected with wild-type strain, the *E. coioides* injected with *L321_RS15240*-RNAi strain exhibited a significantly delay in the time of first death and a significantly decrease in mortality (Fig. 1c). At 4 dpi, the spleens of the *E. coioides* injected with wild-type *P. plecoglossicida* appeared typical symptoms (the surface of the spleen is covered with numerous white spots), only a small number of spleens of the *E. coioides* injected with RNAi strain appeared the typical symptoms, most spleens became red and swollen, no visible white spots were observed (Fig. 1d). Fig. 1e shows the dynamic distribution of the RNAi strain and wild-type *P. plecoglossicida* in *E. coioides*. The difference of abundance between wild-type strain and mutant strain in fish varied with different organs at different times. The abundance of RNAi strain in the spleen and blood was significantly reduced compared with the wild-type *P. plecoglossicida* at most of the time points after injection, and its abundance in the spleen was mostly decreased from 2 to 5 dpi.

Fig. 1f shows the expression level of *L321_RS15240* gene of wild-type *P. plecoglossicida* in spleens at different times post-injection under 18 °C. The expression level of *L321_RS15240* gene in the spleen was

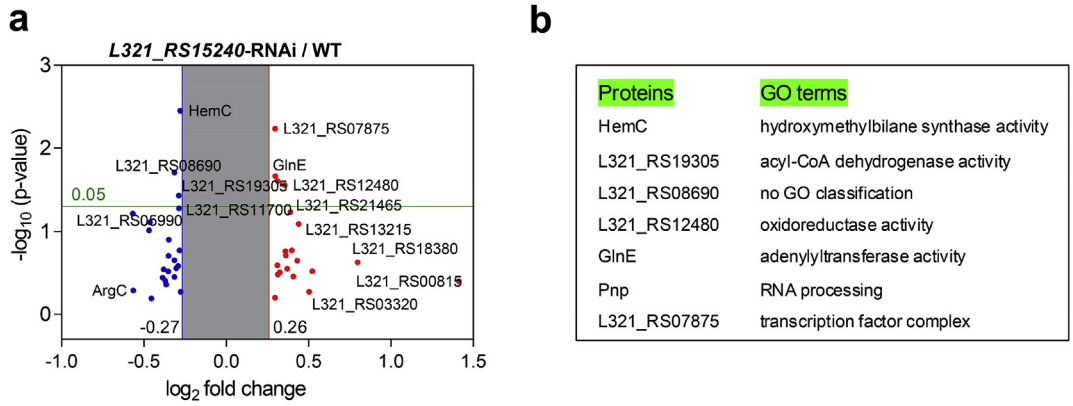

Fig. 2. *L321_RS15240* influences proteome of pathogen. a, Detection of differentially expressed proteins (DEPs) in RNAi strain compared with wild-type strain. **b**, GO functional analyses of the DEPs.

higher than that in the pure culture at all sampling times, the highest expression level was recorded at 1dpi.

3.2. L321_RS15240 influences the expression of protein and mRNA in pathogen

The results of iTRAQ showed that seven proteins were differentially expressed in RNAi strain compared with wild-type strain (Fig. 2a). GO analyses showed the functional classification of differentially expressed proteins (DEPs): biological process (including Pnp), cellular component (including L321_RS07875) and molecular function (including HemC, L321_RS19305, L321_RS12480, GlnE) (Fig. 2b).

Ten mRNAs were was significantly upregulated in RNAi strain compared with wild-type strain (Fig. 3a). Among them, six differentially expressed mRNAs (*DEMs*) obtained GO annotations (Fig. 3a). Interestingly, 11 mRNAs was highly expressed in the wild-type strain from infected-spleens, but their mRNAs were not detected in RNAi strain (Fig. 3b). Furthermore, 9 of the 11 mRNAs were annotated to GO terms (Fig. 3b). RNA-seq results of *P. plecoglossicida* were further confirmed by a qRT-PCR assay (Supplementary Fig. 1).

The above 28 genes (including 7 DEPs, 10 upregulated mRNAs and 11 undetected mRNAs in the RNAi strain infected spleens) were subjected to protein-protein interaction analysis. Among these genes, 15 genes were identified in protein-protein interaction networks (Fig. 3c). The MmsA and RpsB were identified as potentially key genes.

3.3. L321_RS15240 impacts the host response

3.3.1. mRNA expression

After de novo assembly, a total of 55597 unigenes were identified. These unigenes were annotated to 1886 GO terms and 350 KEGG pathways, respectively. The number and expression levels of host DEMs are exhibited in Fig. 4a. Of profiled host mRNAs, 1454 were differentially expressed. Among them, 1218 DEMs were significantly downregulated as a response to the RNAi strain infection, and other 236 DEMs were significantly upregulated. Fig. 4b shows the top 10 significantly enriched GO terms in biological processes of the DEMs, which were related to lipoprotein metabolism and ion homeostasis. The lipoprotein metabolic process was the most significantly enriched GO term. Most of DEMs in this 10 GO terms were significantly upregulated. The significantly enriched pathways from these DEMs involved in immunity, translation and metabolism (Fig. 4c). Interestingly, most of DEMs in all these pathways were significantly upregulated. To identify that the *L321_RS15240* mutation may have the most obvious gene, the top 20 most significantly upregulated and downregulated DEMs were used for protein-protein interaction analysis. The 9 of 40 DEMs were connected to nodes in interaction network (Fig. 4d), all of the 9 DEMs were significantly upregulated. This network was mainly associated with coagulation process, which was consistent with the results of the above KEGG enrichment (Fig. 4c). The F2 was identified as a potentially key gene。

3.3.2. Protein expression

A total of 58 host DEPs were identified, the heatmap showed their expression patterns (Fig. 5a). The DEPs and DEMs expressions of host were not in consistent (Supplementary Fig. 3). A total of 40 significantly enriched GO terms from all DEPs were identified by the GO enrichment analysis. The top 10 enriched GO terms of biological processes were related to assembly and organization of chromatin and metabolism (Fig. 5b), which were different from the above top 10 enriched GO terms from all DEMs. The results clearly indicated that these most obvious GO terms involved in *L321_RS15240* mutation were different between transcriptome and proteome levels. However, as the above host DEMs, most of DEPs in this 10 GO terms were significantly upregulated. Three KEGG pathways in these DEPs were identified as significantly enriched (Fig. 5c), which involved in immunity and metabolism. All DEPs in the phagosome pathway were significantly downregulated. All the DEPs were used for protein-protein interaction analysis. Among these genes, 19 DEPs were identified in protein-protein interaction networks (Fig. 5d). The ISG15 and SPTB was identified as candidate hub proteins affected by the *L321_RS15240* mutation.

3.3.3. Expression of lncRNA and miRNA

A total of 1266 downregulated and 134 upregulated lncRNAs of *E. coioides* were identified by dual RNA-seq. Fig. 6a shows the expression signatures of these differentially expressed lncRNAs (DELs). Fig. 6c shows the expression levels of miRNAs. The qRT-PCR results suggested that RNA-seq data of lncRNAs (Fig. 6b) and miRNAs (Fig. 6d) were accurate and credible.

4. Discussion

Simultaneous monitoring of the host-pathogen interactions through transcriptome and proteome profiling during natural infections can offer a new perspective for understanding of pathogenesis in infection biology [2]. However, to the best of our knowledge, as the bacterial load in infected tissues is the largest obstacle [1,36], research about simultaneously monitor the alterations of transcriptome and proteome of both bacterial pathogen and its host through integrated dual RNA-seq and dual iTRAQ in infected tissue is currently lacking.

DGCs with the GGDEF domain can catalyze synthesis of c-di-GMP [19], which has been shown to regulate the cell cycle, differentiation, virulence, and other cellular functions [20]. In the present study, the RNAi of *L321_RS15240* gene resulted in a decrease in mortality of *E.*

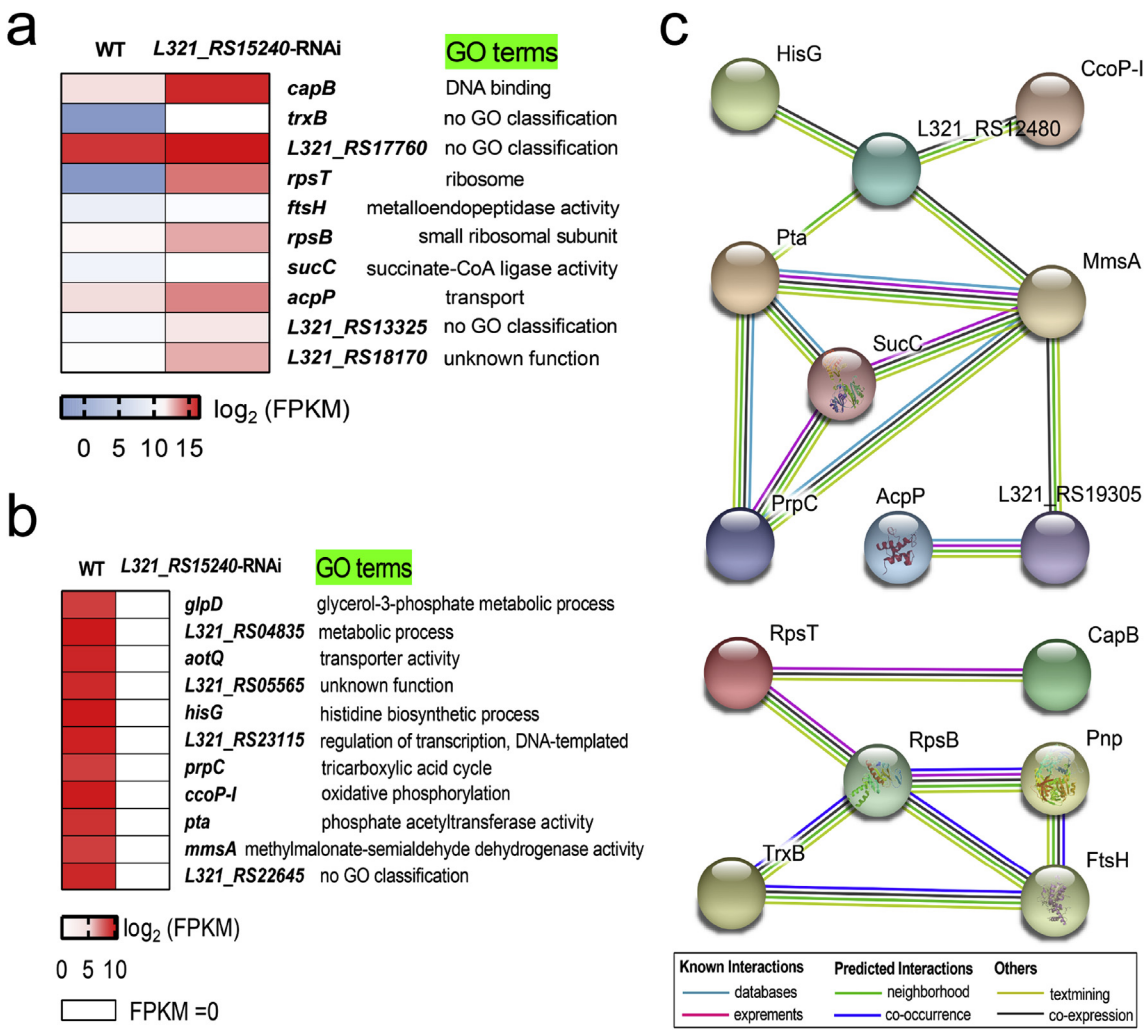

Fig. 3. *L321_RS15240* influences transcriptome of pathogen. a,b, Detection and GO functional analyses of differentially expressed mRNAs (DEMs) in RNAi strain compared with wild-type strain. **c**, Projection of all pathogen DEGs onto the STRING protein-protein interaction network (version 10). Only connected nodes are shown.

coioides infected by RNAi strain of *P. plecoglossicida*. The visible white spots were not observed in most of spleens of *E. coioides* infected by RNAi strain at 4 dpi. Compared with wild type strian, the bacterial load of the RNAi strain of *P. plecoglossicida* in the spleens and blood declined significantly at the most time points after injection. These results indicated that the DGC gene *L321_RS15240* played an important role in pathogenicity of *P. plecoglossicida* against *E. coioides*. Similar observations have been reported by Kulasakara et al. [37], who observed that the infection of mice with the *Pseudomonas aeruginosa* mutant of DGC gene *PA4332* showed a delay in time-to-death and a decline in mortality. In our previous study, the spleen was observed to be the most important target organ [3]. In the present study, the *L321_RS15240* gene in wild-type *P. plecoglossicida* of infected spleens exhibited the highest expression level at 1 dpi, indicating that *L321_RS*15240 had a contribution at early stage of infection in pathogenicity of *P. plecoglossicida* against *E. coioides*. All of these results provide a solid basis for sample selection of dual RNA-seq and dual iTRAQ of tissue and further understanding of the molecular mechanism of *L321_RS15240* in host-pathogen interaction.

Once the pathogen invades its host, the host immune system can rapidly detect and attempt to eliminate them [3,38]. As two closely related and cross-regulated pathways that are responsible for component of innate immune response and hemostasis, the complement and coagulation cascades pathways effectively protect the host by promoting the destruction of pathogens [39,40]. In this study, all the DEMs in the complement and coagulation cascades pathways showing the most significant enrichment was significantly up-regulated. The DEMs (*C8A* and *C8G*) of the complement system were primarily concerned with membrane attack complex that causes lysis of the target cells [41]. The up-regulation of the coagulation factors and fibrinogen in the coagulation system suggested that the RNAi strain infection triggered the activation of the coagulation cascade. Enhanced fibrin deposition can encase the invading bacteria to limit their spread and enhance their clearance [42,43]. Identification of potentially key coagulation factor II (F2) gene in interaction network further indicated that, inhibition of *L321_RS15240* gene on coagulation system may play a most important role in the contribution of this gene to pathogenicity of *P. plecoglossicida*. These results indicated that *L321_RS15240* may control primarily the membrane attack complex and fibrin deposition in inhibition of the *P. plecoglossicida* on the host immune system, especially the inhibition of fibrin deposition. Similar results have been described by Nuss et al. [8], who observed that the most important defense mechanism of the *Yersinia pseudotuberculosis was* also involved with the control of coagulative activities. Meanwhile, as a consequence of the RNAi strain infection, the ribosome, arginine and proline metabolism, and oxidative phosphorylation pathways from transcriptome were also significantly enriched. These three pathways were mainly related to protein synthesis and energy metabolism. The up-regulation

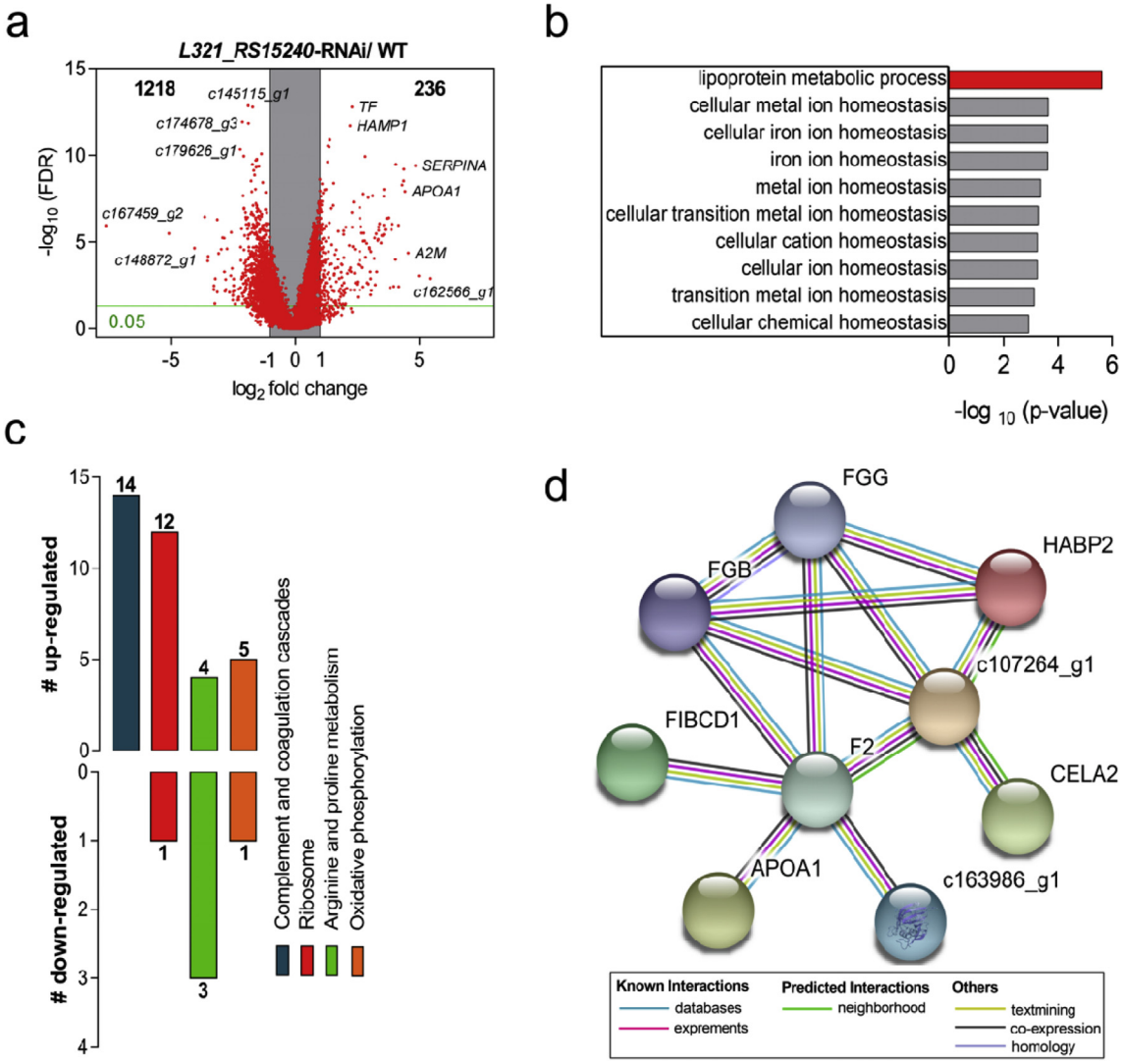

Fig. 4. The host's mRNAs response to RNAi strain. a, Expression levels of host DEMs. **b**, The top 10 significantly enriched GO terms in biological processes of the DEMs. **c**, The significantly enriched pathways from all DEMs. **d**, Projection of the top 20 most significantly upregulated and downregulated DEMs onto the STRING protein-protein interaction network (version 10). Only connected nodes are shown.

of large proportion genes in ribosome and oxidative phosphorylation pathways showed that the protein synthesis and energy metabolism of the host were effectively enhanced after the *L321_RS15240* gene of the pathogen was silenced. In general, amino acids are absorbed and used by the host to synthesize proteins and are oxidized as a source of energy [44]. In this study, the DEMs in arginine and proline metabolism pathway may contribute the protein synthesis and energy metabolism. All the evidence at the mRNA level preliminarily showed the host response to a bacterial infectious pathogen.

Because of complicated post-transcriptional mechanisms and different half-lives of proteins, gene expressions at protein and mRNA levels are not always in consistent [14,45]. In this study, the protein and mRNA expressions of host were not in consistent (Supplementary Fig. 3). This finding is similar with previous observations [46]. In the present study, the host pathways affected by the *L321_RS15240* mutation included in the phagosome pathway and metabolic pathways. These pathways of protein layer were different with the above mRNA layer. The most significant phagosome pathway is involved in phagocytosis, which is a central mechanism in the defense against infectious agents, inflammation and tissue remodeling [47]. The down-regulation of all DEPs in the phagosome pathway may be due to that spread of RNAi strains with weakened virulence was limited by above enhanced fibrin deposition of the extrinsic coagulation cascade. The metabolic pathways involved in metabolism of glutathione, amino sugar and nucleotide sugar. The down-regulation of most of DEPs in the metabolic pathways may simply reflect that *E. coioides* infected by RNAi strain reduced the use of these substances. In all DEPs, the identified candidate hub genes were the ISG15 and SPTB. ISG15 is a ubiquitin-like protein that drives ISG15-dependent cytokine secretion in innate immunity [48]. In this study,the down-regulation of ISG15 may be the result of the induction of weaker virulent RNAi strain. SPTB plays important roles in membrane stability, cell shape and endomembrane traffic [49], its up-regulation may be one of the important reasons for the improvement of survival rate of *E. coioides* infected by RNAi strain. As a result, the integrated dual RNA-seq and iTRAQ of tissue in this study revealed more comprehensive view of host *in vivo* in response to infection. Furthermore, our data provide an overall view of the lncRNA and miRNA expression profile within spleen tissue, which offers a unique resource for the identification of important regulation factors during infection.

The greatest barrier to pathogen transcriptome and proteome sequencing in dual RNA-seq and iTRAQ of *in vivo* for pathogen-host interaction tissue samples is that the abundance of pathogens is too low [8,37]. In this study, we detected the pathogen DEPs and DEMs affected

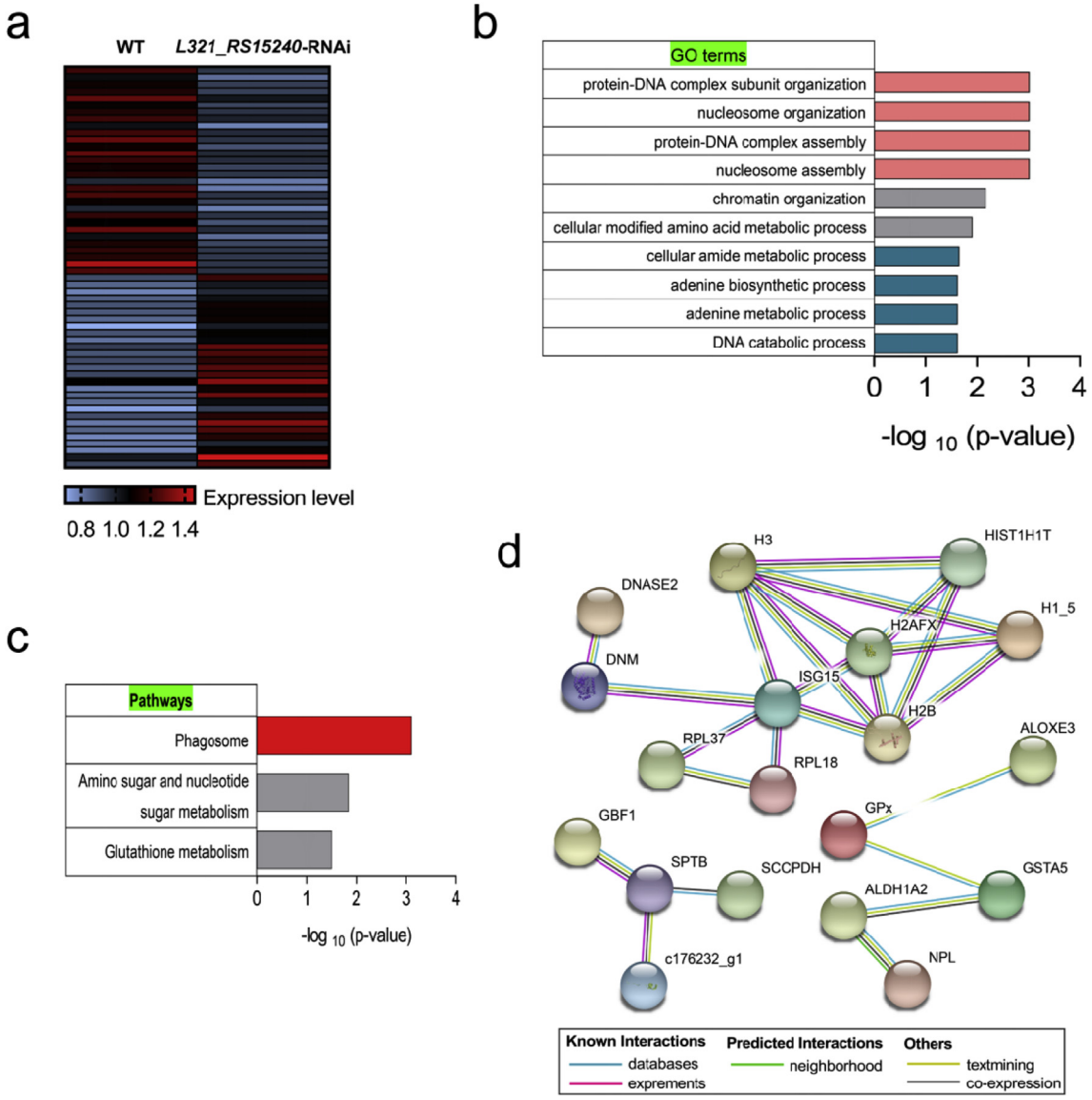

Fig. 5. The host's proteome response to RNAi strain. a, Expression of all the DEPs identified by iTRAQ. **b,c,** GO terms from biological processes (**b**) and KEGG (**c**) enrichment analysis of all the DEPs. **d**, Projection of all the DEPs onto the STRING protein-protein interaction network (version 10). Only connected nodes are shown.

by the *L321_RS15240*-RNAi from the infected spleen samples, which provided a good opportunity to achieve an overall understanding of the pathogenesis of *L321_RS15240* gene during infection. The adaptation of bacterial pathogens metabolism to the nutrients available within the host tissue is a prerequisite of its survival [8]. In this study, most of differentially expressed genes (including DEPs and DEMs) were associated with metabolism. Many of these genes involved in metabolism were strong down-regulation. Such as the porphyrin-containing compound metabolism related gene (*hemc*) at the protein level and the TCA cycle related genes (*prpC* and *ccoP-I*) at the transcript level. These results indicated that *L321_RS15240* may contribute primarily the pathogenicity of *P. plecoglossicida* against *E. coioides* by controlling metabolic process of pathogen. These DEPs and DEMs of pathogen also help to predict the key genes affected by the *L321_RS15240*-RNAi in the infection process. The key gene *mmsA* was significantly down-regulated,which is essential for valine catabolism and associated with central carbon metabolism [50,51]. Furthermore, the interactions between *mmsA* gene and TCA cycle related genes(*prpC* and *ccoP-I*)were found. The results indicated that energy metabolism may play an important role in contribution of *L321_RS15240* for *P. plecoglossicida* pathogenicity. However, the another key gene *rpsB* was significantly up-regulated, which is an essential component of translation machinery [52]. This result showed that,for its own survival in the spleen, RNAi strain enhanced the synthesis and utilization of some proteins under that energy metabolism was suppressed [53]. Another, the *L321_RS15240* may contribute the pathogenicity of *P. plecoglossicida* by controlling virulence genes. For example, the DEP HemC has been shown to affect activity of mucoid phenotype (an important virulence factor) [54]. The DEMs *glpD* has been also shown to regulate cytotoxic effects, a *glpD* mutant exhibited a severely reduced cytotoxicity [55]. Thus, the integrated dual RNA-seq and dual iTRAQ of tissue in this study revealed comprehensive understanding of pathogenic mechanism of *L321_RS15240* in host-pathogen interactions.

5. Conclusion

The DGC gene *L321_RS15240* play an important role in pathogenicity of *P. plecoglossicida.* The *L321_RS15240* affacted the expression of metabolism and virulence related genes at mRNAs and proteins levels of *P. plecoglossicida*. The RNAi of *L321_RS15240* caused changes in mRNAs, lncRNAs, miRNAs and proteins of the host. Association analysis between multiple molecular layers of the pathogen and host

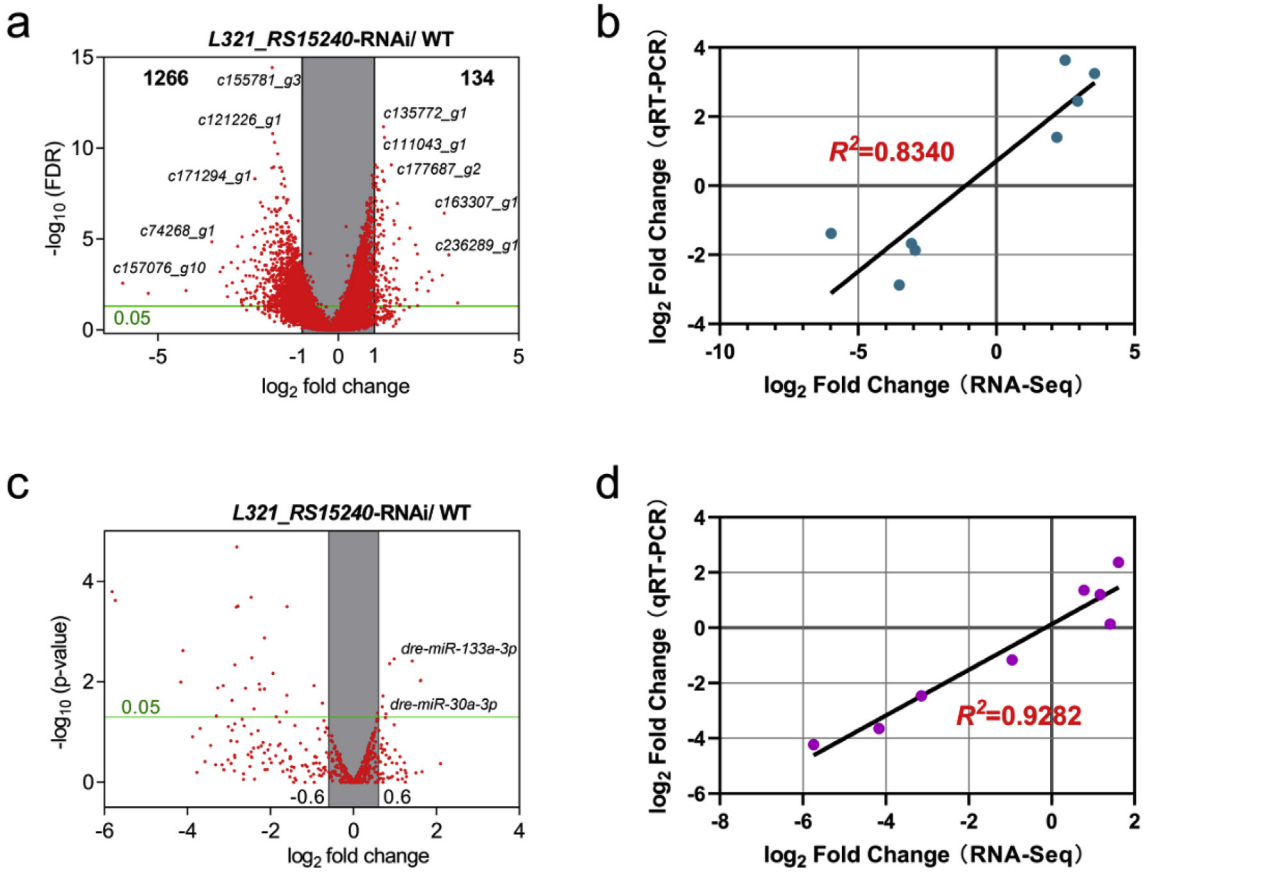

Fig. 6. The host's non-coding RNAs response to RNAi strain. a,c, Volcano plots display the expression profiles of lncRNAs (**a**) and miRNAs (**c**). **b,d**, qRT-PCR validation of the expression of lncRNAs (**b**) and miRNAs (**d**).

deepened the understanding of the molecular mechanism between the pathogen-host interaction. In this study, we provide the first report, to our knowledge, of the successful use of integrated dual RNA-seq and dual iTRAQ of tissue to simultaneously monitor the transcript and protein profiles changes of both pathogen and host in the context of a prokaryotic and eukaryotic biological system.

Declaration of competing interest

The authors declare that the research was conducted in the absence of any commercial or financial relationships that could be construed as a potential conflict of interest.

Acknowledgments

This work was supported by the National Natural Science Foundation of China under contract No. 31672694 and 31972836, and the open fund of Fujian Province Key Laboratory of Special Aquatic Formula Feed under contract No. 2019–01.

Appendix A. Supplementary data

Supplementary data to this article can be found online at https://doi.org/10.1016/j.fsi.2019.11.008.

References

[1] B. Zhang, G. Luo, L. Zhao, et al., Integration of RNAi and RNA-seq uncovers the immune responses of *Epinephelus coioides* to *L321_RS19110* gene of *Pseudomonas plecoglossicida*, Fish Shellfish Immunol. 81 (2018) 121–129, https://doi.org/10.1016/j.fsi.2018.06.051.

[2] Y. Sun, Z. Zhuang, X. Wang, et al., Dual RNA-seq reveals the effect of the *flgM* gene of *Pseudomonas plecoglossicida* on the immune response of *Epinephelus coioides*, Fish Shellfish Immunol. 87 (2019) 515–523, https://doi.org/10.1016/j.fsi.2019.01.041.

[3] R. Tang, L. Zhao, X. Xu, et al., Dual RNA-Seq uncovers the function of an ABC transporter gene in the host-pathogen interaction between *Epinephelus coioides* and *Pseudomonas plecoglossicida*, Fish Shellfish Immunol. 92 (2019) 45–53, https://doi.org/10.1016/j.fsi.2019.05.046.

[4] P.M.J. Beltran, J.D. Federspiel, X. Sheng, et al., Proteomics and integrative omic approaches for understanding host–pathogen interactions and infectious diseases, Mol. Syst. Biol. 13 (3) (2017) 922, https://doi.org/10.15252/msb.20167062.

[5] A.J. Westermann, S.A. Gorski, J. Vogel, Dual RNA-seq of pathogen and host, Nat. Rev. Microbiol. 10 (9) (2012) 618, https://doi.org/10.1038/nrmicro2852.

[6] Y. Sun, G. Luo, L. Zhao, et al., Integration of RNAi and RNA-seq reveals the immune responses of *Epinephelus coioides* to *sigX* gene of *Pseudomonas plecoglossicida*, Front. Immunol. 9 (2018) 1624, https://doi.org/10.3389/fimmu.2018.01624.

[7] R. Aprianto, J. Slager, S. Holsappel, et al., Time-resolved dual RNA-seq reveals extensive rewiring of lung epithelial and pneumococcal transcriptomes during early infection, Genome Biol. 17 (1) (2016) 198, https://doi.org/10.1186/s13059-016-1054-5.

[8] A.M. Nuss, M. Beckstette, M. Pimenova, et al., Tissue dual RNA-seq allows fast discovery of infection-specific functions and riboregulators shaping host–pathogen transcriptomes, Proc. Natl. Acad. Sci. 114 (5) (2017) E791–E800, https://doi.org/10.1073/pnas.1613405114.

[9] Y. Tang, Y. Sun, L. Zhao, et al., Mechanistic insight into the roles of *Pseudomonas plecoglossicida clpV* gene in host-pathogen interactions with *Larimichthys crocea* by dual RNA-seq, Fish Shellfish Immunol. 93 (2019) 344–353, https://doi.org/10.1016/j.fsi.2019.07.066.

[10] L. Wang, Y. Sun, L. Zhao, et al., Dual RNA-seq uncovers the immune response of Larimichthys crocea to the secY gene of Pseudomonas plecoglossicida from the perspective of host-pathogen interactions, Fish Shellfish Immunol. 93 (2019) 949–957, https://doi.org/10.1016/j.fsi.2019.08.040.

[11] U. Fels, K. Gevaert, P. Van Damme, Proteogenomics in aid of host-pathogen interaction studies: a bacterial perspective, Proteomes 5 (4) (2017), https://doi.org/10.3390/proteomes5040026.

[12] A. Harrison, L.G. Dubois, L.S. John-Williams, et al., Comprehensive proteomic and metabolomic signatures of nontypeable Haemophilus influenzae-induced acute otitis media reveal bacterial aerobic respiration in an immunosuppressed environment, Mol. Cell. Proteom. 15 (3) (2016) 1117–1138, https://doi.org/10.1074/mcp.M115.052498.

[13] X. Cao, G. Fan, Y. Dong, et al., Proteome profiling of Paulownia seedlings infected with phytoplasma, Front. Plant Sci. 8 (2017) 342, https://doi.org/10.3389/fpls.

2017.00342.
[14] D. Greenbaum, C. Colangelo, K. Williams, et al., Comparing protein abundance and mRNA expression levels on a genomic scale, Genome Biol. 4 (9) (2003) 117, https://doi.org/10.1186/gb-2003-4-9-117.
[15] M. Li, K. Wang, S. Li, et al., Exploration of rice pistil responses during early post-pollination through a combined proteomic and transcriptomic analysis, J. Proteom. 131 (2016) 214–226, https://doi.org/10.1016/j.jprot.2015.11.004.
[16] L. Huang, W. Liu, Q. Jiang, et al., Integration of transcriptomic and proteomic approaches reveals the temperature-dependent virulence of *Pseudomonas plecoglossicida*, Front. Cell. Infect. Microbiol. 8 (2018) 207 https://10.3389/fcimb.2018.00207.
[17] L. Huang, Y. Zuo, Q. Jiang, et al., A metabolomic investigation into the temperature-dependent virulence of *Pseudomonas plecoglossicida* from large yellow croaker (*Pseudosciaena crocea*), J. Fish Dis. 42 (3) (2019) 431–446, https://doi.org/10.1111/jfd.12957.
[18] J.T. Zhang, S.M. Zhou, S.W. An, et al., Visceral granulomas in farmed large yellow croaker, *Larimichthys crocea* (Richardson), caused by a bacterial pathogen, *Pseudomonas plecoglossicida*, J. Fish Dis. 37 (2) (2014) 113–121, https://doi.org/10.1111/jfd.12075.
[19] P.D. Newell, S. Yoshioka, K.L. Hvorecny, et al., Systematic analysis of diguanylate cyclases that promote biofilm formation by Pseudomonas fluorescens Pf0-1, J. Bacteriol. 193 (18) (2011) 4685–4698 https://10.1128/JB.05483-11.
[20] U. Römling, M.Y. Galperin, M. Gomelsky, Cyclic di-GMP: the first 25 years of a universal bacterial second messenger, Microbiol. Mol. Biol. Rev. 77 (1) (2013) 1–52 https://10.1128/MMBR.00043-12.
[21] L. Huang, Y. Zhang, R. He, et al., Phenotypic characterization, virulence, and immunogenicity of Pseudomonas plecoglossicida rpoE knock-down strain, Fish Shellfish Immunol. 87 (2019) 772–777 https://10.1016/j.fsi.2019.02.028.
[22] B. Zhang, Z. Zhuang, X. Wang, et al., Dual RNA-Seq reveals the role of a transcriptional regulator gene in pathogen-host interactions between *Pseudomonas plecoglossicida* and *Epinephelus coioides*, Fish Shellfish Immunol. 87 (2019) 778–787, https://doi.org/10.1016/j.fsi.2019.02.025.
[23] G. Luo, L. Huang, Y. Su, et al., flrA, flrB and flrC regulate adhesion by controlling the expression of critical virulence genes in Vibrio alginolyticus, Emerg. Microb. Infect. 5 (8) (2016) e85 https://10.1038/emi.2016.82.
[24] G. Luo, X. Xu, L. Zhao, et al., *clpV* is a key virulence gene during in vivo *Pseudomonas plecoglossicida* infection, J. Fish Dis. 42 (7) (2019) 991–1000, https://doi.org/10.1111/jfd.13001.
[25] W. Chen, L. Yi, S. Feng, et al., Characterization of microRNAs in orange-spotted grouper (Epinephelus coioides) fin cells upon red-spotted grouper nervous necrosis virus infection, Fish Shellfish Immunol. 63 (2017) 228–236 https://10.1016/j.fsi.2017.02.031.
[26] B. Langmead, S.L. Salzberg, Fast gapped-read alignment with Bowtie 2, Nat. Methods 9 (4) (2012) 357 https://10.1038/NMETH.1923.
[27] M.G. Grabherr, B.J. Haas, M. Yassour, et al., Full-length transcriptome assembly from RNA-Seq data without a reference genome, Nat. Biotechnol. 29 (7) (2011) 644 https://10.1038/nbt.1883.
[28] X. Song, G. Liu, Z. Huang, et al., Temperature expression patterns of genes and their coexpression with LncRNAs revealed by RNA-Seq in non-heading Chinese cabbage, BMC Genomics 17 (1) (2016) 297 https://10.1186/s12864-016-2625-2.
[29] A. Conesa, S. Götz, J.M. García-Gómez, et al., Blast2GO: a universal tool for annotation, visualization and analysis in functional genomics research, Bioinformatics 21 (18) (2005) 3674–3676 https://10.1093/bioinformatics/bti610.
[30] M.D. Robinson, D.J. McCarthy, G.K. Smyth, edgeR: a Bioconductor package for differential expression analysis of digital gene expression data, Bioinformatics 26 (1) (2010) 139–140 https://10.1093/bioinformatics/btp616.
[31] M.I. Love, W. Huber, S. Anders, Moderated estimation of fold change and dispersion for RNA-seq data with DESeq2, Genome Biol. 15 (12) (2014) 550 https://10.1186/s13059-014-0550-8.
[32] C. Wang, B. Gong, P.R. Bushel, et al., The concordance between RNA-seq and microarray data depends on chemical treatment and transcript abundance, Nat. Biotechnol. 32 (9) (2014) 926 https://10.1038/nbt.3001.
[33] H. Ouyang, Z. Wang, X. Chen, et al., Proteomic analysis of chicken skeletal muscle during embryonic development, Front. Physiol. 8 (2017) 281 https://10.3389/fphys.2017.00281.
[34] H. Yu, X. Wang, J. Xu, et al., iTRAQ-based quantitative proteomics analysis of molecular mechanisms associated with Bombyx mori (Lepidoptera) larval midgut response to BmNPV in susceptible and near-isogenic strains, Journal of proteomics 165 (2017) 35–50 https://10.1016/j.jprot.2017.06.007.
[35] D. Szklarczyk, A. Franceschini, S. Wyder, et al., STRING v10: protein–protein interaction networks, integrated over the tree of life, Nucleic Acids Res. 43 (D1) (2014) D447–D452 https://10.1093/nar/gku1003.
[36] U. Fels, K. Gevaert, P. Van Damme, Proteogenomics in aid of host–pathogen interaction studies: a bacterial perspective, Proteomes 5 (4) (2017) 26 https://10.3390/proteomes5040026.
[37] H. Kulesekara, V. Lee, A. Brencic, et al., Analysis of Pseudomonas aeruginosa diguanylate cyclases and phosphodiesterases reveals a role for bis-(3′-5′)-cyclic-GMP in virulence, Proc. Natl. Acad. Sci. 103 (8) (2006) 2839–2844 https://10.1073/pnas.0511090103.
[38] F. Martinon, A. Mayor, J. Tschopp, The inflammasomes: guardians of the body, Annu. Rev. Immunol. 27 (2009) 229–265 https://10.1146/annurev.immunol.021908.132715.
[39] J. Cohen, The immunopathogenesis of sepsis, Nature 420 (6917) (2002) 885 https://10.1038/nature01326.
[40] R. Silasi-Mansat, H. Zhu, N.I. Popescu, et al., Complement inhibition decreases the procoagulant response and confers organ protection in a baboon model of Escherichia coli sepsis, Blood 116 (6) (2010) 1002–1010 https://10.1182/blood-2010-02-269746.
[41] M.S. Ray, O. Moskovich, O. Iosefson, et al., Mortalin/GRP75 binds to complement C9 and plays a role in resistance to complement-dependent cytotoxicity, J. Biol. Chem. 289 (21) (2014) 15014–15022 https://10.1074/jbc.M114.552406.
[42] T. van der Poll, H. Herwald, The coagulation system and its function in early immune defense, Thromb. Haemost. 112 (04) (2014) 640–648 https://10.1160/TH14-01-0053.
[43] F. Guinet, P. Ave, S. Filali, et al., Dissociation of tissue destruction and bacterial expansion during bubonic plague, PLoS Pathog. 11 (10) (2015) e1005222https://10.1371/journal.ppat.1005222.
[44] Y. Liu, X. Wang, Y. Hou, et al., Roles of amino acids in preventing and treating intestinal diseases: recent studies with pig models, Amino Acids 49 (8) (2017) 1277–1291 https://10.1007/s00726-017-2450-1.
[45] P. Lan, W. Li, W. Schmidt, Complementary proteome and transcriptome profiling in phosphate-deficient Arabidopsis roots reveals multiple levels of gene regulation, Mol. Cell. Proteom. 11 (11) (2012) 1156 https://10.1074/mcp.M112.020461.
[46] M.P. Washburn, K. Antonius, O. Guy, et al., Protein pathway and complex clustering of correlated mRNA and protein expression analyses in Saccharomyces cerevisiae, Proc. Natl. Acad. Sci. U.S.A. 100 (6) (2003) 3107–3112 https://10.1073/pnas.0634629100.
[47] L.M. Stuart, R.A.B. Ezekowitz, Phagocytosis: elegant complexity, Immunity 22 (5) (2005) 539–550 https://10.1016/j.immuni.2005.05.002.
[48] C.D. Swaim, A.F. Scott, L.A. Canadeo, et al., Extracellular ISG15 signals cytokine secretion through the LFA-1 integrin receptor, Mol. Cell 68 (3) (2017) 581–590 https://10.1016/j.molcel.2017.10.003.
[49] G.H. Mazock, A. Das, C. Base, et al., Transgene rescue identifies an essential function for Drosophila beta spectrin in the nervous system and a selective requirement for ankyrin-2-binding activity, Mol. Biol. Cell 21 (16) (2010) 2860 https://10.1091/mbc.E10-03-0180.
[50] M.I. Steele, D. Lorenz, K. Hatter, et al., Characterization of the mmsAB operon of Pseudomonas aeruginosa PAO encoding methylmalonate-semialdehyde dehydrogenase and 3-hydroxyisobutyrate dehydrogenase, J. Biol. Chem. 267 (19) (1992) 13585–13592.
[51] P.R. Kohler, E.L. Choong, S. Rossbach, The RpiR-like repressor IolR regulates inositol catabolism in Sinorhizobium meliloti, J. Bacteriol. 193 (19) (2011) 5155–5163 https://10.1128/JB.05371-11.
[52] L.V. Aseev, A.O. Chugunov, R.G. Efremov, et al., A single missense mutation in a coiled-coil domain of Escherichia coli ribosomal protein S2 confers a thermosensitive phenotype that can be suppressed by ribosomal protein S1, J. Bacteriol. 195 (1) (2013) 95–104 https://10.1128/JB.01305-12.
[53] P.G. Jones, M. Mitta, Y. Kim, et al., Cold shock induces a major ribosomal-associated protein that unwinds double-stranded RNA in *Escherichia coli*, Proc. Natl. Acad. Sci. U.S.A. 93 (1) (1996) 76–80 https://10.1073/pnas.93.1.76.
[54] C.D. Mohr, S.K. Sonsteby, V.J.M. Deretic, The *Pseudomonas aeruginosa* homologs of hemC and hemD are linked to the gene encoding the regulator of mucoidy AlgR, Mol. Gen. Genet. 242 (2) (1994) 177–184 https://10.1007/BF00391011.
[55] C. Hames, S. albedel, M. oppert, et al., Glycerol metabolism is important for cytotoxicity of Mycoplasma pneumoniae, J. Bacteriol. 191 (3) (2009) 747–753 https://10.1128/JB.01103-08.